DOI:10.1021/jf903793p

JOURNAL OF AGRICULTURAL AND FOOD CHEMISTRY
ARTICLE

Inhibition of Epidermal Growth Factor Receptor Signaling by *Saussurea involucrata*, a Rare Traditional Chinese Medicinal Herb, in Human Hormone-Resistant Prostate Cancer PC-3 Cells

Tzong-Der Way,[†,◆] Jang-Chang Lee,[‡,§,◆] Daih-Huang Kuo,[⊥] Ling-Ling Fan,[†] Chi-Hung Huang,[#] Hui-Yi Lin,[‡] Po-Chuen Shieh,[⊥] Po-Tsun Kuo,[▽] Chien-Fu Liao,[∥] Hanshi Liu,[○] and Jung-Yie Kao*[,▽]

[†]Department of Biological Science and Technology, College of Life Sciences, [‡]School of Pharmacy, College of Pharmacy, [§]Graduate Institute of Pharmaceutical Chemistry, and [∥]School of Chinese Medicine, College of Chinese Medicine, China Medical University, Taichung, Taiwan, [⊥]Department of Pharmacy and Graduate Institute of Pharmaceutical Technology, College of Pharmacy and Health Care, Tajen University, Pingtung, Taiwan, [#]Taiwan Advance Biopharm, Inc., Xizhi City, Taipei, Taiwan, [▽]Institute of Biochemistry, College of Life Science, National Chung Hsing University, Taichung, Taiwan, and [○]Dalian Practical Biotechnology Co., Dalian, People's Republic of China. [◆]Contributed equally to this work.

Prostate carcinoma is the most frequently diagnosed malignancy and the second leading cause of death of men in the United States. To date, no effective therapeutic treatment allows abrogation of the progression of prostate cancer to more invasive forms. In this study, we identified *Saussurea involucrata* Kar. et Kir., a rare traditional Chinese medicinal herb, as a potential agent for androgen-independent prostate cancer patients and investigated its biological mechanism as an antineoplastic agent. *S. involucrata* caused a concentration- and time-dependent inhibition of cell proliferation in human hormone-resistant prostate cancer PC-3 cells. Moreover, in vitro studies in a panel of several types of human cancer cell lines revealed that *S. involucrata* inhibited cell proliferation with high potency. To evaluate the bioactive compounds, we successively extracted the *S. involucrata* with fractions of methanol (SI-1), ethyl acetate (SI-2), *n*-butanol (SI-3), and water (SI-4). Among these extracts, SI-2 contains the most effective bioactivity. SI-2 treatment resulted in significant time-dependent growth inhibition together with G1 phase cell cycle arrest and apoptosis in PC3 cells. In addition, SI-2 treatment strongly induced p21*WAF1/CIP* and p27*KIP1* expression, independent of the p53 pathway, and downregulated expression of cyclin D1 and cyclin-dependent kinase 4 (CDK4). SI-2 treatment increased levels of Bax, cytochrome *c*, activated caspase-3, and active caspase-9 and decreased Bcl-2 expression level. One of the major targets for the therapy in prostate cancer can be epidermal growth factor receptor (EGFR). SI-2 markedly reduced phosphorylation of EGFR and inhibited activation of AKT and STAT3. Moreover, p.o. administration of SI-2 induced a dose-dependent inhibition of PC-3 tumor growth in vivo. In summary, our study identifies *S. involucrata* as an effective inhibitor of EGFR signaling in human hormone-resistant prostate cancer PC-3 cells. We suggest that *S. involucrata* could be developed as an agent for the management of EGFR-positive human cancers.

KEYWORDS: *Saussurea involucrata*; EGFR; AKT; STAT3; prostate cancer

INTRODUCTION

Saussurea involucrata Kar. et Kir., known as snow lotus, grows in the mountains on rocky habitats 2600 m in elevation or higher in the Tian Shan and A'er Tai areas in China. Because of excessive harvesting of the wild plants that are used in pharmaceutical preparations and its very slow growth, the wild population of this plant has been threatened with depletion in recent years. *S. involucrata* is now almost extinct and has been listed as a second grade national protected wild plant in China (*1*). On the basis of the theories of traditional Chinese medicine, it has the effects of warming the kidney, activating "yang", expelling wind, eliminating dampness, inducing menstruation, and promoting blood circulation. In folk medicine, it is used for the treatment of rheumatoid arthritis, impotence, irregular menses, cough with cold, stomachache, and altitude sickness, among others (*2*).

Prostate cancer is the sixth most commonly diagnosed cancer in the world. It is also the second leading cause of cancer-related death among men in America (*3*). To date, no effective therapeutic treatment allows the abrogation of its progression to more invasive disease forms. Although most prostate cancer initially remains sensitive to androgen for therapeutic treatment, many patients die of androgen-independent prostate cancer within a few years (*4*).

*To whom correspondence should be addressed. Tel: 886-4-22840468, ext. 222. Fax: 886-4-2285-3487. E-mail: jykao@dragon.nchu.edu.tw.

 Published on Web 02/18/2010

Future improvements in prostate cancer treatments are likely to come from novel agents targeting molecular pathways that promote tumor cell growth and survival. Recently, novel therapeutic approaches targeting the epidermal growth factor receptor (EGFR) superfamily and their downstream pathways have been generated (*5*). EGFR is a 170 kDa glycoprotein consisting of an extracellular ligand-binding domain, a transmembrane tail containing a single hydrophobic anchor sequence, and an intracellular domain containing tyrosine kinase activity. Upon ligand binding, EGFR may either homodimerize or heterodimerize and is capable of phosphorylating itself (autophosphorylation) as well as other proteins (transphosphorylation) (*6*). The tyrosine-phosphorylated EGFR then serves as a docking site for a variety of adaptor proteins and enzymes involved in the recruitment and activation of downstream intracellular-signaling cascades to initiate the activation of downstream pathways, including the activation of phosphatidylinositol 3-kinase (PI3K)/AKT and/or the activation of Raf/Ras/mitogen-activated protein kinase (MAPK) cascades. EGFR downstream pathways lead to cell proliferation, migration, adhesion, antiapoptosis, angiogenesis, and metastasis (*7*). EGFR is frequently overexpressed in prostate cancer, and this is associated with a more aggressive clinical outcome (*8*). In addition, EGFR and its ligand, EGF, play a critical role during tumorigenesis of the prostate gland (*9*), and EGFR signaling has been linked to the progression of androgen-responsive prostate cancer to androgen-independent tumors (*10*).

Cell cycle control plays a principal role in cell differentiation, proliferation, and cell growth. Progression through the cell cycle is regulated by CDKs, whose activity is inhibited by the CDK inhibitors. Cyclins, CDKs, and CDK inhibitors are frequently deregulated in cancers (*11*). Activation of cyclin/CDK activities is required for cell cycle progression and G1/S transition in response to growth factor stimulation. Several studies have demonstrated that growth factors trigger cascades of intracellular signals that lead to activation of nuclear transcriptional factors that activate cyclin/CDK complexes; active cells pass the G1 checkpoint and embark on DNA replication in the S phase (*12*). G1/S transition is positively controlled by two families of CDKs, including the complexes of CDK2/cyclin E and cyclin A or the complexes of cyclin-dependent kinase 4 (CDK4)/cyclin D or CDK6/cyclin D. In response to the growth factors, the cyclin D/CDK4/6 complexes induce the phosphorylation of retinoblastoma (Rb) protein and dissociate from E2F, which triggers G1 cell cycle progression (*13*).

The upregulation of CDK inhibitors is frequently responsible for the inhibition of G1 cell cycle progression and for withdrawal from the cell cycle. CDK inhibitors can be subdivided into two families, including the INK4 family, consisting of p16*INK4a*, p15*INK4b*, p18*INK4c*, and p19*INK4d*, and KIP/CIP families consisting of p21*WAF1*/*CIP*, p27*KIP1*, and p57*KIP2*. The p21*WAF1*/*CIP* is a target for diverse signals, which cause cell growth arrest and promote differentiation. Introduction of p21*WAF1*/*CIP* protein into human untransformed and malignant cells induces cell cycle arrest (*14*). The kinase activities of the CDK complexes are negatively regulated by CDK inhibitors, such as p21*WAF1*/*CIP*, which blocks cell cycle progression by binding and inactivating the cyclin−CDK complex system (*14*). A mutation in p21*WAF1*/*CIP* that specifically abrogated binding to CDKs was identified in cells isolated from a primary breast tumor (*15*), suggesting that p21*WAF1*/*CIP* has tumor-suppressive activity.

In China, Korea, and Japan, Complementary and Alternative Medicine (CAM) therapies such as traditional Chinese medicine have been an option to cancer patients for centuries, whereas in Europe and North America, CAM has been growing in popularity only in the past few decades. In this study, we identified *S. involucrata* as a potential agent for CAM and investigated its biological mechanism as an antineoplastic agent for androgen-independent prostate cancer patients. Our results clearly show that treatment of PC-3 cells with *S. involucrata* had a very potent inhibitory effect on the phosphorylation and activation of EGFR and on the AKT and STAT3 pathway. Our results may thus offer therapeutic advantages in the treatment and prevention of human prostate cancer.

MATERIALS AND METHODS

Materials. Rutin, Z-VAD-FMK, thymidine, SB203580, propidium iodide (PI), MTT [3-(4,5-dimethylthiazol-2-yl)-2,5-diphenyl tetrazolium bromide], and antibodies for Bcl-2, Bax, caspase 9, caspase 3, and β-actin were purchased from Sigma (St. Louis, MO). Hispidulin was purchased from Tocris Bioscience (Bristol, United Kingdom). Antibodies for STAT3, EGFR, AKT, p-AKT, ERK, c-jun N-terminal kinase (JNK), p53, and p21*WAF1*/*CIP* were purchased from Cell Signaling Technology (Beverly, MA). Antibodies for p-ERK, p-STAT3, p38, p-p38, p27*KIP1*, cytochrome *c*, CDK2, CDK4, cyclin E, and cyclin D1 were obtained from Santa Cruz Biotechnology (Santa Cruz, CA). The antibody for p-EGFR (Y38) was obtained from Abcam (Cambridge, MA). Antibodies for mouse and rabbit conjugated with horseradish peroxidase were purchased from Chemicon (Temecula, CA). Western Chemiluminescent HRP Substrate was from Millipore Corp. (Billerica, MA).

Preparation of Fractions. The wild plant of *S. involucrata* used in this study was a gift from Biopure Biotechnology (Changhua, Taiwan). Twenty grams of dried and powdered aerial parts, including flower, of *S. involucrate* was extracted with 100 mL of methanol three times under reflux for 2 h, respectively. The methanol extracts (SI-1) were combined, and the solvent was evaporated in vacuo to give a deep brown syrup. The syrup was resuspended in water and then partitioned successively with pentane, ethyl acetate (SI-2) and *n*-butanol (SI-3) to leave a water layer (SI-4). The solvents were evaporated respectively, and the residues were used throughout this study.

Reverse-Phase High-Performance Liquid Chromatography (HPLC) Analysis of Flavonoids in *S. involucrata*. The determination of flavonoids from *S. involucrata* was carried out by HPLC with a photodiary detector. The HPLC system consisted of a Shimadzu LC-20AT solvent delivery system, equipped with a SPD-M20A photodiode array detector, set at 270 nm. Samples were injected with SiL-20A autosample to separate on the TSK-Gel ODS-100S column. The column was maintained at an ambient temperature of 25 °C. The flow rate of the system was 1.0 mL/min. The mobile phase consisted of solvent A (0.3% formic acid) and solvent B (acetonitrile). The elution profile for A was 0−10 min, with a linear gradient change of 0−5%; 10−40 min, with a linear gradient change to 55%; and maintained for another 10 min with a post run time to equilibrate the column and for the baseline to return to the normal and initial working conditions.

Cell Culture. Cells were purchased from the American Type Culture Collection (Manassas, VA). MDA-MB-231 and SKOV3 were grown in DMEM/F-12 (Invitrogen, Carlsbad, CA) supplemented with 10% fetal bovine serum (FBS) (Invitrogen) and 1% penicillin−streptomycin (Invitrogen). HepG2, SAS, and Cal-27 were cultured in DMEM (Invitrogen) containing 10% FBS (Invitrogen) and 1% penicillin−streptomycin (Invitrogen). PC3 and LNCaP were cultured in RPMI-1640 (Invitrogen) containing 10% FBS (Invitrogen) and 1% penicillin−streptomycin (Invitrogen). Cells were grown in a humidified incubator at 37 °C under 5% CO_2 in air.

Cell Proliferation Assays. As described previously (*16*), the effects of osthole and taxol on cell proliferation were examined by MTT method.

Cell-cycle synchronization. Synchronization of PC3 cells was performed by double thymidine block. Briefly, cells were treated with 3 mM thymidine in medium/10% FCS for 16 h and washed twice with PBS and then cultured in fresh medium/10% FCS for 10 h. The cells were treated again with medium/10% FCS containing 3 mM thymidine for 16 h. After the cells were washed with PBS, the block was released by the incubation of cells in fresh medium/10% FCS (indicated as time zero), and the cells were harvested at 0, 12, 24, 48, and 72 h. The cell cycle progression was detected by flow cytometric analysis.

Cell Cycle Analysis. Cells (5×10^5) were cultured in 6 mm cell culture dish and incubated for 24 h. Cells were then harvested in a 15 mL tube, washed with PBS, resuspended in PBS, and fixed in 2 mL of iced 100% ethanol at −20 °C overnight. Cell pellets were collected by centrifugation, resuspended in 0.5 mL of hypotonic buffer (0.5% Triton X-100 in PBS and 0.5 μg/mL RNase), and incubated at room temperature for 30 min. Subsequently, 1 mL of PI solution (50 μg/mL) was added, and the mixture was allowed to stand on ice for 30 min. Fluorescence emitted from the propidium iodide−DNA complex was quantitated after the fluorescent dye was excited by FAC-Scan cytometry (BD Biosciences, San Jose, CA).

Western Blot Analysis. Cells (1.5×10^6) were seeded onto a 100 mm tissue culture dish containing 10% FBS DMEM/F12 and cultured for 24 h. Then, cells were incubated in 10% FBS DMEM/F12 treating with various agents as indicated in figure legends. After treatment, cells were placed on ice, washed with cold PBS, and lysed in lysis buffer. Western Blot was done as described previously (*17*). The intensity of the bands was scanned and quantified with NIH image software.

Cytochrome *c* Release. Mitochondrial and cytosolic fractions were prepared by resuspending cells in ice-cold buffer A [250 mM sucrose, 20 mM HEPES, 10 mM KCl, 1.5 mM MgCl2, 1 mM EDTA, 1 mM EGTA, 1 mM DTT, 17 mg/mL PMSF, 8 mg/mL aprotinin, and 2 mg/mL leupeptin (pH 7.4)]. Cells were passed through a 27G needle 10 times. Unlysed cells and nuclei were pelleted by centrifugation for 10 min at 750*g*. The supernatant was then centrifuged at 100000*g* for 15 min. The pellet was resuspended in buffer A and represented the mitochondrial fraction. The supernatant was centrifuged again at 100000*g* for 1 h. The final supernatant represented the cytosolic fraction.

In Vivo Studies. Male BALB/c nude mice (18−20 g; 4−6 weeks of age) were purchased from National Animal Center (Taipei, Taiwan) and maintained in a pressurized ventilated cage according to institutional regulations. PC3 cells in log phase growth (5×10^6 cells) were inoculated subcutaneously into the right flank of the mice. When tumors reached an approximate volume of 100 mm^3, mice were selected and distributed for drug studies. The ethyl acetate extract of *S. involucrata* was diluted with sterile saline before injection. Mice were weighed, and tumors were measured using calipers every 3 days. Tumor volumes were determined by measuring the length (l) and the width (w), and the volumes were calculated as $V = lw^2/2$. On the final day of the treatment, mice were sacrificed, tumors were excised, weighed, and sectioned, and the tumor sections were embedded in OCT (optimum cutting temperature) compound and frozen at −70 °C.

Short Hairpin RNA. RNAi reagents were obtained from the National RNAi Core Facility located at the Institute of Molecular Biology/Genomic Research Center, Academia Sinica, supported by the National Research Program for Genomic Medicine Grants of NSC (NSC 97-3112-B-001-016). Short hairpin RNAs (shRNAs) were designed to target specific sequences of human p27*KIP1* (clone ID: NM 004064; target sequence: 5′-AGCAATGCGCAGGAATAAGG-3′) and p21*WAF1*/*CIP* (clone ID: NM 000389; target sequence: 5′-GTCACTGTCTTG-TACCCTTGT-3′). One day before transfection, cells were seeded without antibiotics with a density of 30−40%. A 20 nM concentration of shRNAs was transfected into cells by lipofectamine 2000 (Invitrogen). Cells were incubated for an additional 24 h, and SI-2 was added as previously described. After another 24 h, the cells were analyzed by flow cytometry and Western blot as previously described.

Tranfection. One day before transfection, 2×10^5 cells without serum and antibiotics were plated in six-well plates. PC3 cells were grown to 90% confluence and transfected on the following day by Lipofectamine™ 2000 (Invitrogen), premixed plasmid DNA with OPTI-MEM (Gibco, Carlsbad, CA) for 5 min and then added to each well. After 24 h of incubation, the transfection was completed.

Statistical Analysis. All values were expressed as mean ± standard errors (SEs). Each value was the mean of at least three separate experiments in each group, and Student's t test was used for statistical comparison.

RESULTS

***S. involucrata* Inhibited Hormone-Resistant Prostate Cancer PC-3 Cell Proliferation.** The exposure of human hormone-resistant prostate cancer PC-3 cells to *S. involucrata* caused a concentration- and time-dependent inhibition of cell proliferation. *S. involucrata* also displayed a similar effect in several types of human cancer cell lines, including breast cancer MDA-MB-231 cells, ovarian cancer SKOV3 cells, hepatocellular carcinoma HepG2 cells, and oral cancer SAS and Cal-27 cells (**Figure 1A**). To evaluate the bioactive compounds, we successively extracted the *S. involucrata* with fractions of methanol (SI-1), ethyl acetate (SI-2), *n*-butanol (SI-3), and water (SI-4) (**Figure 1B**). PC3 cells were treated with different *S. involucrata* extracts, and a decrease in cell proliferation was detected by MTT assay. The IC_{50} values (in μg/mL at 24 h) of SI-1, SI-2, SI-3, and SI-4 were 55.45, 50.95, >200, and 138.04, respectively. Among these extracts, SI-2 contains the most effective *S. involucrata* ingredients that reduce cell proliferation in our assay (**Figure 1B**). Next, to evaluate the antiproliferative effect of *S. involucrata* in androgen-sensitive prostate cancer LNCaP cells, SI-2 exhibited less of an effect on LNCaP cells (**Figure 1C**). Our result showed that *S. involucrata* exhibited potent antiproliferative activity against hormone-resistant prostate cancer cells.

***S. involucrata* Altered Cell Cycle Progression and Induced Apoptosis in PC3 Cells.** To detect the cell cycle progression, PC3 cells were synchronized at the G1/S phase by using double thymidine block. Upon release from the block, more than 80% of the cells progressed into S and G2/M phases (0−6 h) (data not shown). In the presence of 50 μg/mL SI-2 (the half maximal inhibitory concentration as assessed by MTT assay), the cell cycle progression was almost completely blocked, and the population of apoptotic cells increased after a 24 h release from double thymidine block (**Figure 2**).

***S. involucrata*-Induced Cell Cycle Arrest Is Associated with Upregulation of p21*WAF1*/*CIP* and p27*KIP1*.** The effect of SI-2 on the induction of p21*WAF1*/*CIP* and p27*KIP1*, which regulate progression of the cell cycle at the G1−S phase transition checkpoint, was examined using immunoblotting. Immunoblot analysis revealed that treatment of PC3 cells with SI-2 resulted in significant time-dependent induction of p21*WAF1*/*CIP* and p27*KIP1* as compared with untreated cells (**Figure 3A**). However, under similar experimental conditions, expression of the p53 tumor suppressor protein was unaffected, suggesting that it is unlikely that p53 is involved in the cell cycle arrest induced by *S. involucrata*. Moreover, ablation of p21*WAF1*/*CIP* or p27*KIP1* production using shRNA had a recoverable effect on *S. involucrata*-inhibited PC-3 cell proliferation (**Figure 3B**). These results suggested that *S. involucrata*-induced accumulation of p21*WAF1*/*CIP* and p27*KIP1*, independent of the p53 pathway, may also be responsible for the G1 phase arrest in PC3 cells.

***S. involucrata* Altered Cell Cycle Regulatory Proteins in PC3 Cells.** To determine whether *S. involucrata*-induced growth inhibition of PC3 cells was due to decreased activation of the cell cycle machinery, expression of cell cycle regulatory molecules was examined using immunoblotting assays. As shown in **Figure 3C**, there was a notable decrease in the steady-state levels of cyclin D1 in PC3 cells. However, there was no change in the protein expression of cyclin E. Cyclin D1 serves as the regulatory subunit of CDK4 and contributes to its stability. Next, we assessed the effects of SI-2 on CDKs protein expression. Treatment of PC3 cells with SI-2 resulted in a time-dependent decrease in protein expression of CDK4. Nevertheless, there was no change in the protein expression of CDK2 (**Figure 3D**).

Effect of *S. involucrata* on the Expression of Bcl-2 Family and the Cleavage and Activation of Caspase in PC3 Cells. Several gene products are known to be important in controlling the apoptotic process. The imbalance of expression of anti- and proapoptotic proteins after stimulation is one of the major mechanisms underlying the ultimate fate of cells in the apoptotic process (*18*). We examined the expression of proapoptosis proteins, Bax, at different time points in SI-2-treated cells. As shown in **Figure 4A**, there

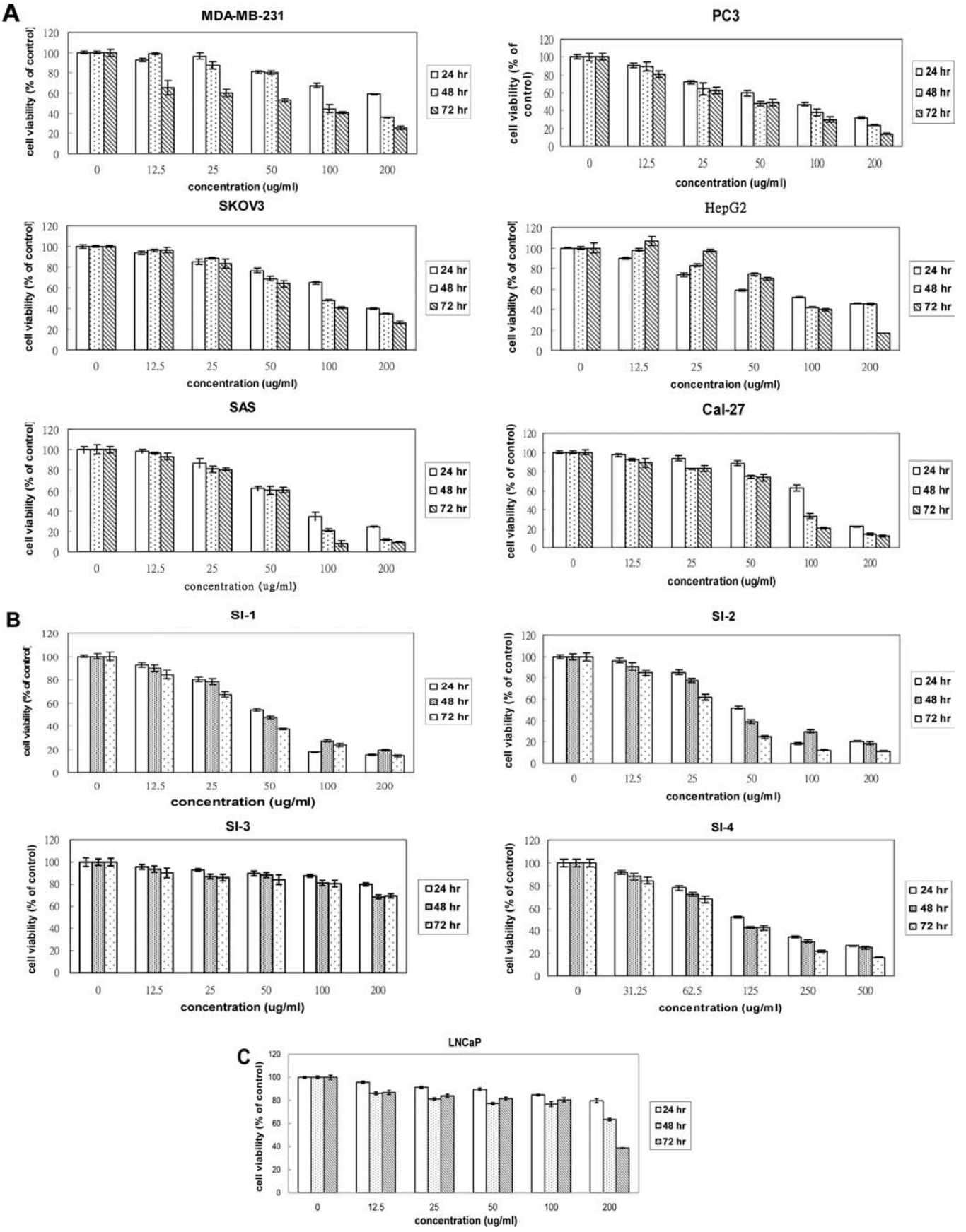

Figure 1. Proliferation−inhibitory effect of *S. involucrata* on various human cancer cell lines. (**A**) MDA-MB-231, PC3, SKOV3, HepG2, SAS, and Cal-27 cells were treated with indicated concentrations of *S. involucrata* for the indicated time. (**B**) PC3 cells were treated with indicated concentrations of SI-1, SI-2, SI-3, and SI-4 for the indicated time. (**C**) LNCaP cells were treated with indicated concentrations of SI-2 at the indicated time. The cell viability was then determined using MTT assay. This experiment was repeated three times. The bar represents the SE.

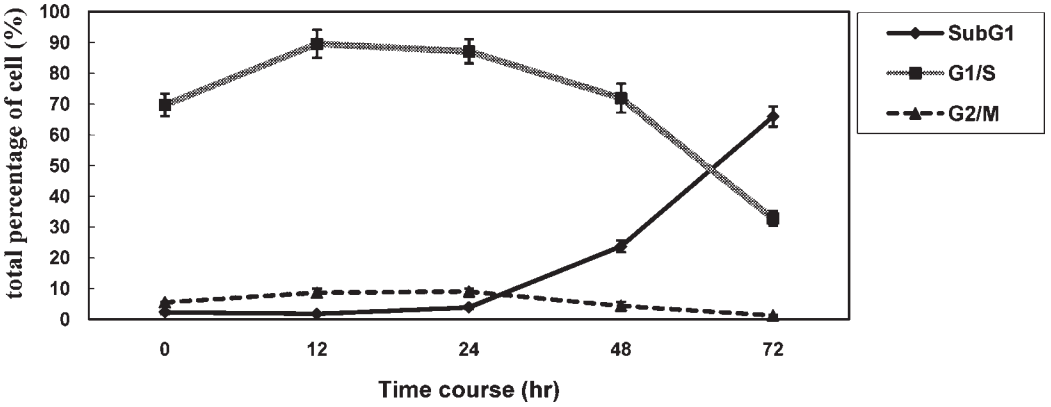

Figure 2. Effect of *S. involucrata* on cell cycle progression in human prostate cancer PC3 cells. Synchronization of PC3 cells was performed by double thymidine block as described in the Materials and Methods. Then, the cells were released in the absence or presence of 50 μg/mL SI-2. This experiment was repeated three times. The bar represents the SE.

was a marked increase of Bax expression in SI-2-treated PC3 cells. We next examined the expression of antiapoptotic proteins, Bcl-2, of various times after SI-2 treatment. The exposure of PC3 cells to 50 μg/mL SI-2 resulted in downregulation of Bcl-2 (**Figure 4A**). The release of cytochrome *c* from the mitochondria is the central gate in turning on apoptosis. This release is regulated by the interaction of proapoptotic proteins, including Bid, Bax, and Bak, and antiapoptotic proteins, including Bcl-2 and Bcl-XL (*10*). We next tested whether SI-2 also induced cytochrome *c* release. **Figure 4B** clearly shows that SI-2 led to the release of cytochrome *c* into the cytosol in a time-dependent manner. Subsequent to the release of cytochrome *c*, caspases play a central role in mediating various apoptotic responses. To monitor the enzymatic activity of caspases during SI-2-induced apoptosis, we carried out immunoblotting and found that cleavage patterns of caspase-9 (**Figure 4C**) and caspase-3 (**Figure 4D**) were observed in PC3 cells at the dosage of 50 μg/mL SI-2 in a time-dependent manner. Consistent with this finding, the caspase inhibitor Z-VAD-FMK significantly inhibited the *S. involucrata*-inhibited PC-3 cell proliferation in a dose-dependent manner (**Figure 4E**).

***S. involucrata* Inhibited Constitutive Activation of EGFR, Phosphorylation of AKT, and STAT3 in PC3 Cells.** Aberrant expression and/or activation of EGFR have been reported in prostate cancer and provide a strong rationale for targeting this growth factor receptor for EGFR-positive human cancers. We determined the effect of SI-2 in hormone-resistant prostate cancer PC-3 cells. Using phosphospecific antibodies that detect specific tyrosine residues of EGFR at the 38 sites, SI-2 treatment resulted in a time-dependent decrease in the phosphorylation of EGFR (**Figure 5**). The signaling pathways induced by activated EGFR include PI3K/AKT and STAT3, both of which play a significant role in the mitogenic and cell survival responses mediated by the EGFR. We next evaluated the effect of SI-2 treatment to PC3 cells on the phosphorylation of AKT and STAT3. We found that SI-2 treatment inhibited phosphorylation of AKT and STAT3 in a time-dependent manner (**Figure 6A**).

AKT and STAT3 Overexpression Leads to Resistance to *S. involucrat* Inhibited PC3 Cell Proliferation. If AKT and STAT3 were critical targets of *S. involucrata*, profound expression of AKT and STAT3 should attenuate *S. involucrata*-inhibited cell proliferation. To assess this hypothesis, we did an AKT and STAT3-overexpression experiment using cDNA of CA-AKT and CA-STAT3. As a result, the SI-2-treated AKT and STAT3-overexpressing cells showed no enhanced inhibition of cell proliferation, in comparison with the control (**Figure 6B**), suggesting that *S. involucrata* might target, at least in part, AKT and STAT3 in the PC3 cells.

Effects of *S. involucrata* on ERK, JNK, and p38 Activation in PC3 Cells. To determine whether *S. involucrata* affects MAPK activation, time−course experiments, measuring ERK1/2, JNK and p38 activation in response to SI-2, were performed in PC3 cells. Cells were exposed to SI-2 for various incubation times. **Figure 6C** shows an immunoblot of SI-2-treated cells using antibodies specific for phosphorylated ERK1/2, JNK, and p38. The results of these experiments indicated that ERK1/2 and JNK were not significantly activated by SI-2. However, SI-2 increased the amount of phosphorylated p38 at 12 h. To test whether *S. involucrata* inhibits cell growth via activation of the p38 pathways, PC3 cells were exposed to SI-2 for 24 h in the absence or presence of SB203580, a specific inhibitor of p38. As shown in **Figure 6D**, treatment with SB203580 had no recovered effect on cell growth inhibition of SI-2. These results suggest that an increase of the amount of phosphorylated p38 has no significant effect in *S. involucrata* inhibiting cell growth.

Antitumor Activity of *S. involucrata* in Human Prostate Xenografts. *S. involucrata* was identified as a potent and selective antitumor agent in human prostate carcinoma. To investigate the in vivo antitumor activity of *S. involucrata*, we carried out xenografts with PC3 cells in nude mice. Nude mice were implanted s.c. with PC3 cells, randomized, and divided into three groups. The control group was treated with saline, and the treated groups were given p.o. three times a week with SI-2 (10 and 30 mg/kg). Animals monitored for vital signs and weight changes for the duration of the experiment did not lose weight (**Figure 7C**). After 4 weeks, the animals were killed, and no pathologic signs were seen. As shown in **Figure 7A**, p.o. administration of SI-2 induced a dose-dependent inhibition of PC-3 tumor growth (30 mg/kg SI-2, 1123.93 mm^3, $P < 0.01$ versus vehicle; vehicle-treated group = 2483.28 mm^3 on day 28). Moreover, p.o. administration of SI-2 induced a dose-dependent inhibition of PC-3 tumor weight (**Figure 7B**).

Profile of Constituents in SI-2 Extracts. *S. involucrata* is an important medicinal plant that produces a few bioactive secondary metabolites, such as hispidulin, rutin, and syringin (*19*). To analyze the detailed compositions of the SI-2, HPLC was used. The HPLC chromatograms for the mixture of hispidulin, rutin, and syringin (**Figure 8A**) and SI-2 (**Figure 8B**) were illustrated. As shown in **Figure 8B**, SI-2 involved hispidulin and rutin. Interestingly, the active flavonoid, syringin, was not detectable in SI-2. It is likely that other bioactive molecules exist in *S. involucrata*.

DISCUSSION

For thousands of years, *S. involucrata* has been used extensively as a free radical scavenging, antifatigue, anti-inflammation,

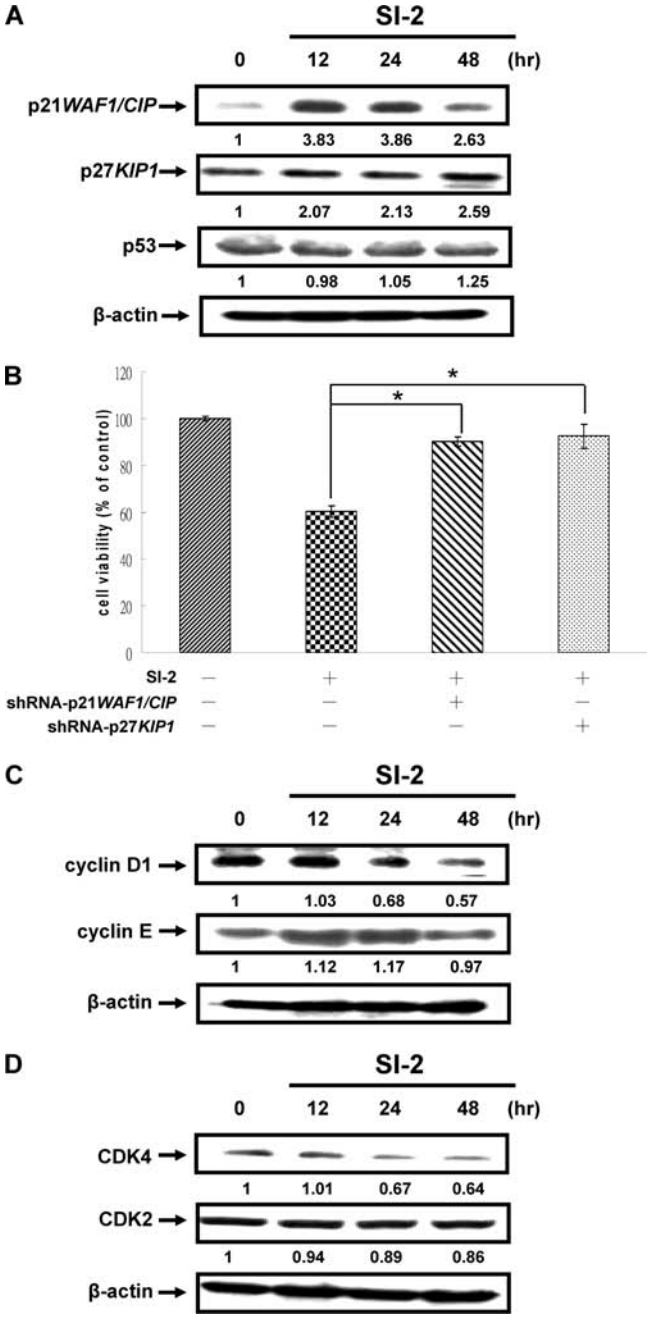

Figure 3. *S. involucrata* alters cell cycle regulatory proteins in PC3 cells. PC3 cells were treated with a vehicle (DMSO) or SI-2 (50 μg/mL) for the indicated time. Cells were then harvested and lysed for the detection of (**A**) p21*WAF1/CIP*, p27*KIP1*, p53, and β-actin, (**C**) cyclin D1, cyclin E, and β-actin, and (**D**) CDK2, CDK4, and β-actin protein expression. Western blot data presented are representative of those obtained in at least three separate experiments. The values below the figures represent a change in protein expression of the bands normalized to β-actin. (**B**) PC3 cells were transfected with 50 nmol/L p21*WAF1/CIP* or p27*KIP1*-shRNA. Twenty-four hours after transfection, cells were treated with SI-2 (50 μg/mL) for 24 h. The cell viability was then determined using the MTT assay. This experiment was repeated three times. The bar represents the SE, and the asterisk indicates that the values are significantly different from the control (*$p < 0.05$).

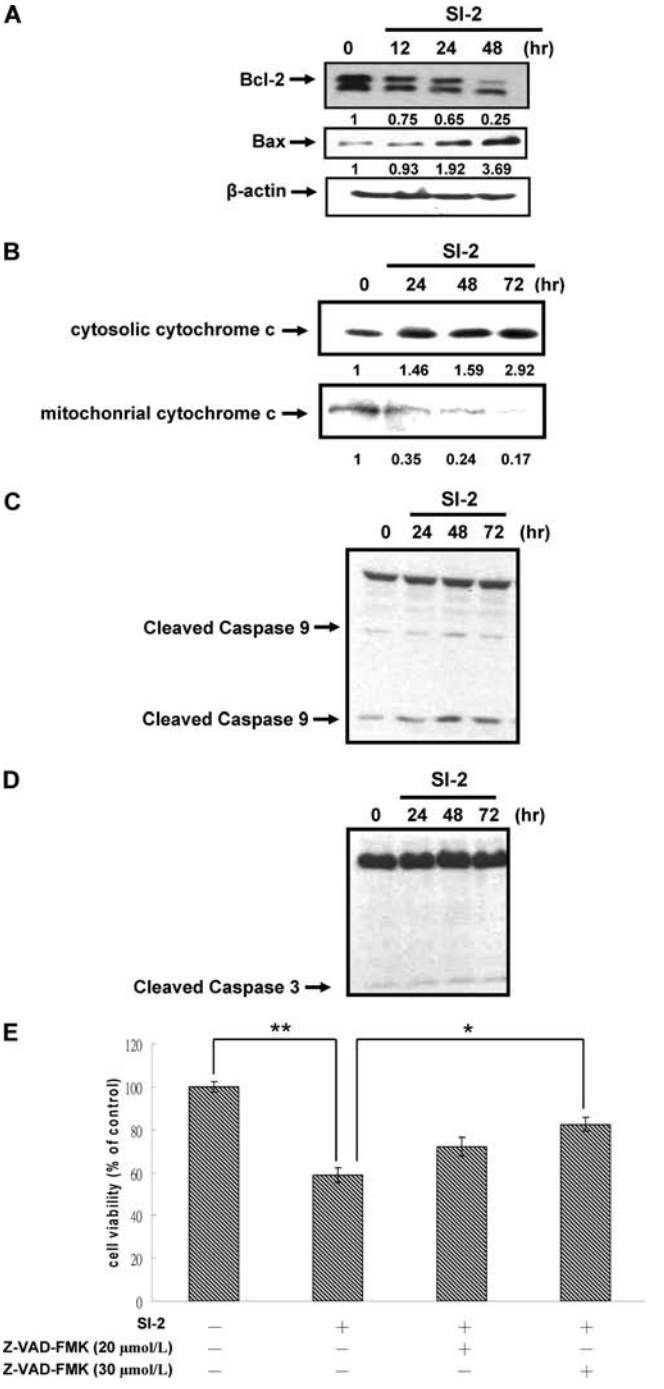

Figure 4. Effect of *S. involucrata* on apoptosis-related proteins in PC3 cells. PC3 cells were treated with a vehicle (DMSO) or SI-2 (50 μg/mL) for the indicated time. Cells were then harvested and lysed for the detection of (**A**) Bcl2, Bax, and β-actin, (**B**) cytochrome *c* in the mitochondrial and cytosolic fraction, (**C**) caspase-9, and (**D**) caspase-3 protein expression. Western blot data presented are representative of those obtained in at least three separate experiments. The values below the figures represent the change in protein expression of the bands normalized to β-actin. (**E**) Z-VAD-FMK or the vehicle (DMSO) was added to the medium at 1 h before the SI-2 (50 μg/mL) treatment. After the 24 h incubation, the PC3 cell viability was determined using MTT assay. This experiment was repeated three times. The bar represents the SE, and the asterisk indicates that the values are significantly different from the control (*$p < 0.05$; **$p < 0.01$).

anticancer, and immunomodulation treatment in China (*20*). Whereas *S. involucrata* has been approved for cancer therapy in China, its biology and mechanism of action in treating cancer are not well understood. In the present study, we have investigated the effects of *S. involucrata* on the biology of tumor cells. *S. involucrata* exerted growth inhibition on several cancer cell lines. Specifically, *S. involucrata* inhibited the viability of human

hormone-resistant prostate cancer PC-3 cells at low IC_{50} values, suggesting that it has a powerful cytotoxic effect. In this work, we demonstrated that *S. involucrata* induced suppression of serum-activated EGFR activity and its mediated downstream pathways, AKT and STAT3, in PC3 cells.

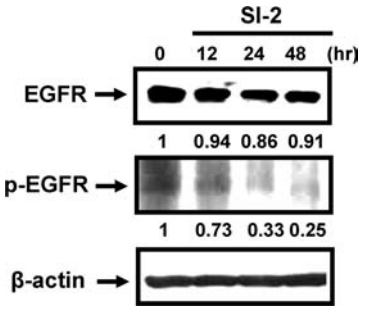

Figure 5. Effect of *S. involucrata* on the constitutive autoposphorylation of EGFR. PC3 cells were treated with a vehicle (DMSO) or SI-2 (50 μg/mL) for the indicated time. Cells were then harvested and lysed for the detection of EGFR, p-EGFR, and β-actin protein expression. Western blot data presented are representative of those obtained in at least three separate experiments. The values below the figures represent the change in protein expression of the bands normalized to β-actin.

Our studies demonstrated that *S. involucrata* strongly inhibited PC3 cell growth and proliferation and blocked cell cycle progression at the G1/S phase transition. To better understand the molecular mechanisms underlying *S. involucrata*-induced cell growth inhibition and cell cycle arrest, we determined the effect of *S. involucrata* on the expression of key regulatory proteins that are required for transition past the G1/S phase restriction point of cell cycle progression. Indeed, we found that *S. involucrata* caused G1 phase cell cycle arrest together with a decrease in cyclin D1/CDK4, which are involved in cell cycle progression from the G1 to S phase. Our results were similar to present studies (*21*, *22*). Chiang et al. identified that antroquinonol, a well-known traditional Chinese medicine for treatment of liver diseases, displayed effective anticancer activity against both HBV DNA-positive and -negative HCC cell lines. The authors identified that the mRNA expressions of the G1 regulator proteins were not modified by antroquinonol, indicating an inhibition of translational but not transcriptional levels. Antroquinonol inhibited cellular G1 regulator protein synthesis through inhibition of protein phosphorylation including mTOR, p70S6K, and 4E-BP1 (*21*).

It has been well-established that p21*WAF/CIP1* and p27*KIP1* as the negative controllers play important roles in the regulation of cell cycle progression (*23*). Our results demonstrated that a significant upregulation in p21*WAF1/CIP* and p27*KIP* occurred

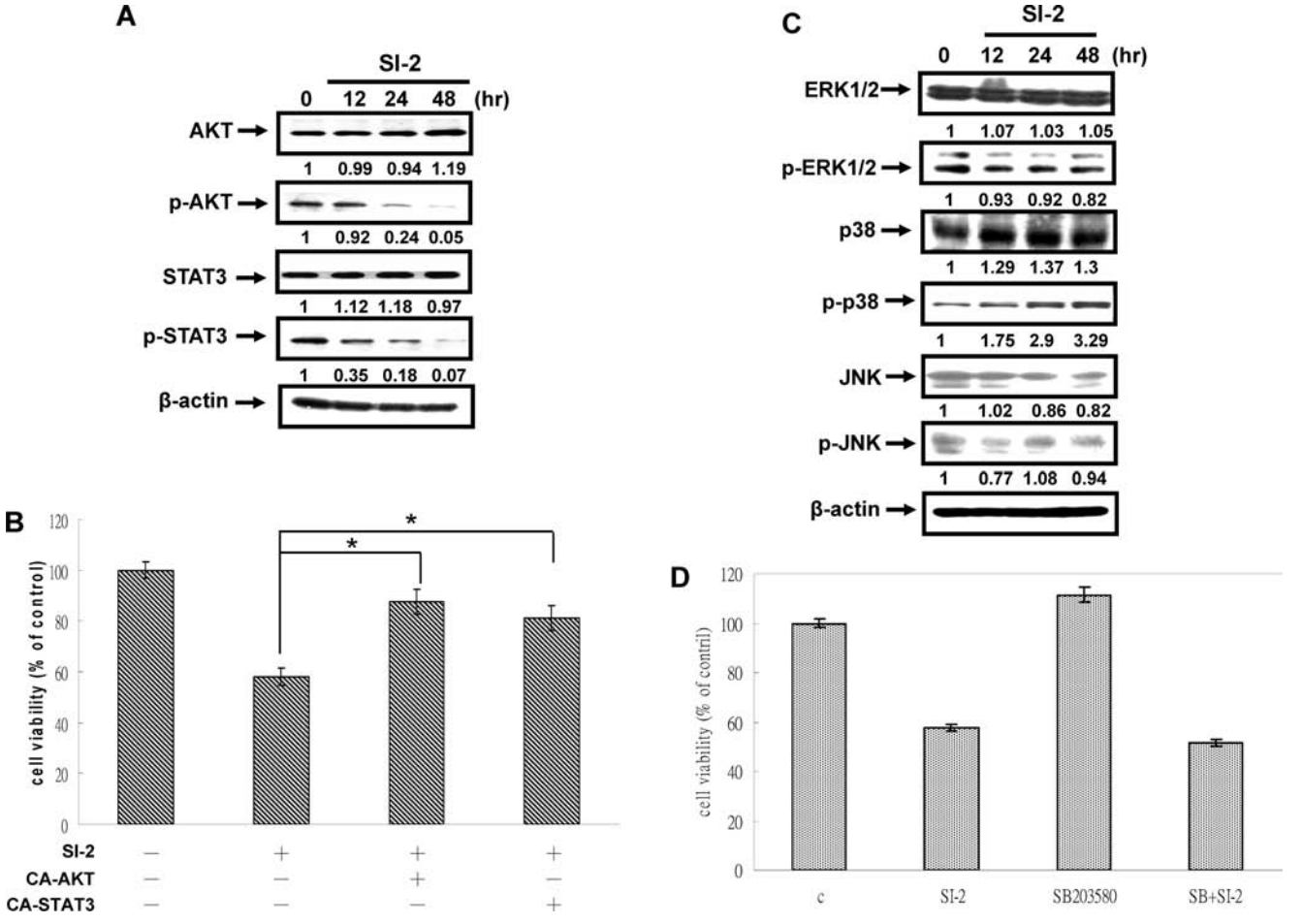

Figure 6. Effect of *S. involucrata* on the EGFR signaling. PC3 cells were treated with a vehicle (DMSO) or SI-2 (50 μg/mL) for the indicated time. Cells were then harvested and lysed for the detection of (**A**) AKT, p-AKT, STAT3, p-STAT3, and β-actin and (**C**) ERK1/2, p-ERK1/2, p38, p-p38, JNK, p-JNK, and β-actin protein expression. Western blot data presented are representative of those obtained in at least three separate experiments. The values below the figures represent the change in protein expression of the bands normalized to β-actin. (**B**) PC3 cells were transfected with 50 nmol/L CA-Akt or CA-STAT3. Twenty-four hours after transfection, cells were treated with SI-2 (50 μg/mL) for 24 h. Then, the cell viability was determined using the MTT assay. (**D**) PC3 cells were cultured with SI-2 (50 μg/mL) or p38 inhibitor (SB203580) in the absence or presence of SI-2. Then, the cell viability was determined using MTT assay. This experiment was repeated three times. The bar represents the SE.

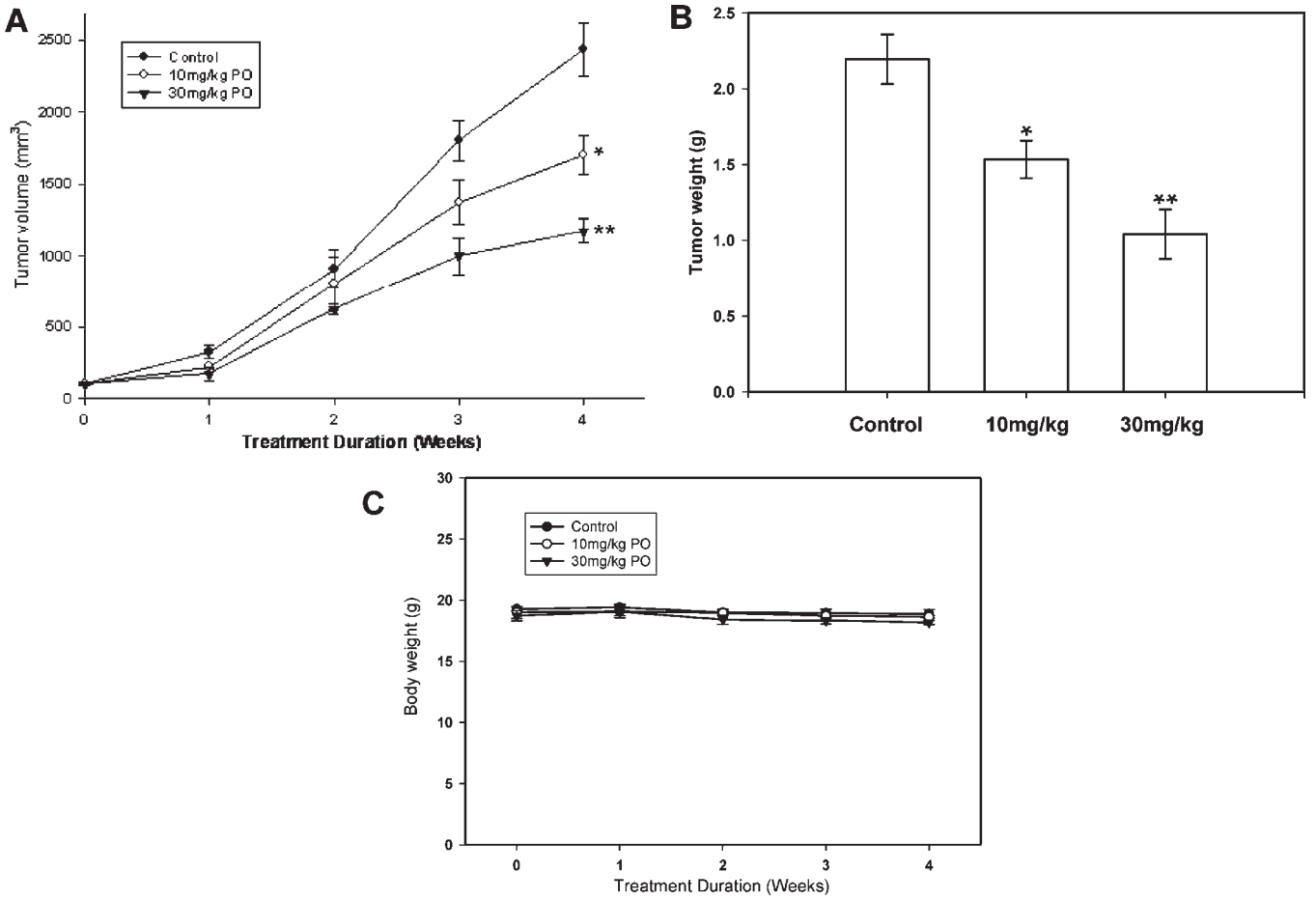

Figure 7. Effect of *S. involucrata* on antitumor activity. PC3 cells were used to establish xenografts in male BALB/c nude mice. Animals (six mices/group) were given control or SI-2 (10 and 30 mg/kg) by given p.o. injection 3 times/week. (**A**) Tumor volume (mm^3), (**B**) tumor weight (g), and (**C**) body weight (g). The bar represents the SE, and the asterisk indicates that the values are significantly different from the control (*$p < 0.05$; **$p < 0.01$).

during the G1 phase arrest in PC3 cells treated with *S. involucrata*. Moreover, ablation of p21*WAF1*/*CIP* or p27*KIP1* production using shRNA had a recoverable effect on *S. involucrata*-inhibited PC-3 cell proliferation. Interestingly, however, *S. involucrata* had no effect on the expression of p53 as determined by immunoblot analysis, suggesting that *S. involucrata*-induced accumulation of p21*WAF1*/*CIP*, independent of the p53 pathway, may also be responsible for the G1 phase arrest in PC3 cells.

The ratio between antiapoptotic (Bcl-2) and proapoptotic (Bax) proteins/molecules has been suggested as a primary event in determining the sensitivity to apoptosis through destabilization of the mitochondrial membrane and activation of caspase cascade (*24*). Bax binds to the mitochondrial membrane and induces cytochrome *c* release that subsequently activates caspase-3 leading to downstream apoptotic responses (*25*). Inhibition of EGFR has been shown to result in a marked decrease in Bcl-2 and Bcl-XL levels and a marked increase in the expression of Bak and Bax, which are known to heterodimer with Bcl-2 or Bcl-XL to favor apoptosis (*26*). The present study suggests that *S. involucrata* treatment of PC3 cells resulted in induction of apoptosis via modulation of Bcl-2 family members and activation of caspase 3.

Therapeutic targeting on EGFR has been intensely investigated. Numerous reports document the significance of EGFR in prostate cancer progression (*9*, *10*). In recent years, considerable enthusiasm was generated for EGFR inhibitors as targeted agents for cancer treatment. It is widely appreciated that those agents that can modulate EGFR signaling pathways in cancer cells that overexpress EGFR may be able to affect the steady state cell population and may be useful in the management and therapy of cancer. This notion assumes importance because in EGFR overexpressing cancer cells a balance between proliferation and apoptosis is lost that has been implicated in a cellular mass and tumor progression. Consistent with this notion, there is a need to develop novel dietary-based agents for the management of EGFR-positive human cancers. Therefore, we determined whether *S. involucrata* treatment inhibits constitutive autoposphorylation of EGFR. Data presented here suggest that *S. involucrata* treatment to EGFR-positive cells PC3 cells resulted in a time-dependent decrease in the phosphorylation of EGFR. To achieve this claim, additional cells lines have been selected for evaluation of *S. involucrata*-induced EGFR phosphorylation blockade. Our data show that *S. involucrate* potently inhibited constitutive autoposphorylation of EGFR (data no shown).

The signaling pathways induced by activated EGFR include the PI3K/AKT and STAT3, both of which play a significant role in the mitogenic and cell survival responses mediated by EGFR (*27*). PI3K is a dimer enzyme composed of an inhibitory/regulatory (p85) and a catalytic (p110) subunit. The p85 subunit anchorage to erbB receptor docking sites, and p110 subunit is responsible for the phosphorylation and activation of the protein serine/threonine kinase AKT (*28*). STAT3, which is believed to be associated with transforming growth factor (TGF)-β and EGFR signaling, is constitutively activated in many human cancers (*29*). The activation of PI3K/AKT and STAT3 pathways contributes to tumor resistance to targeted therapeutics as well as to chemo/radiation therapy. Therefore, inhibition of PI3K/AKT

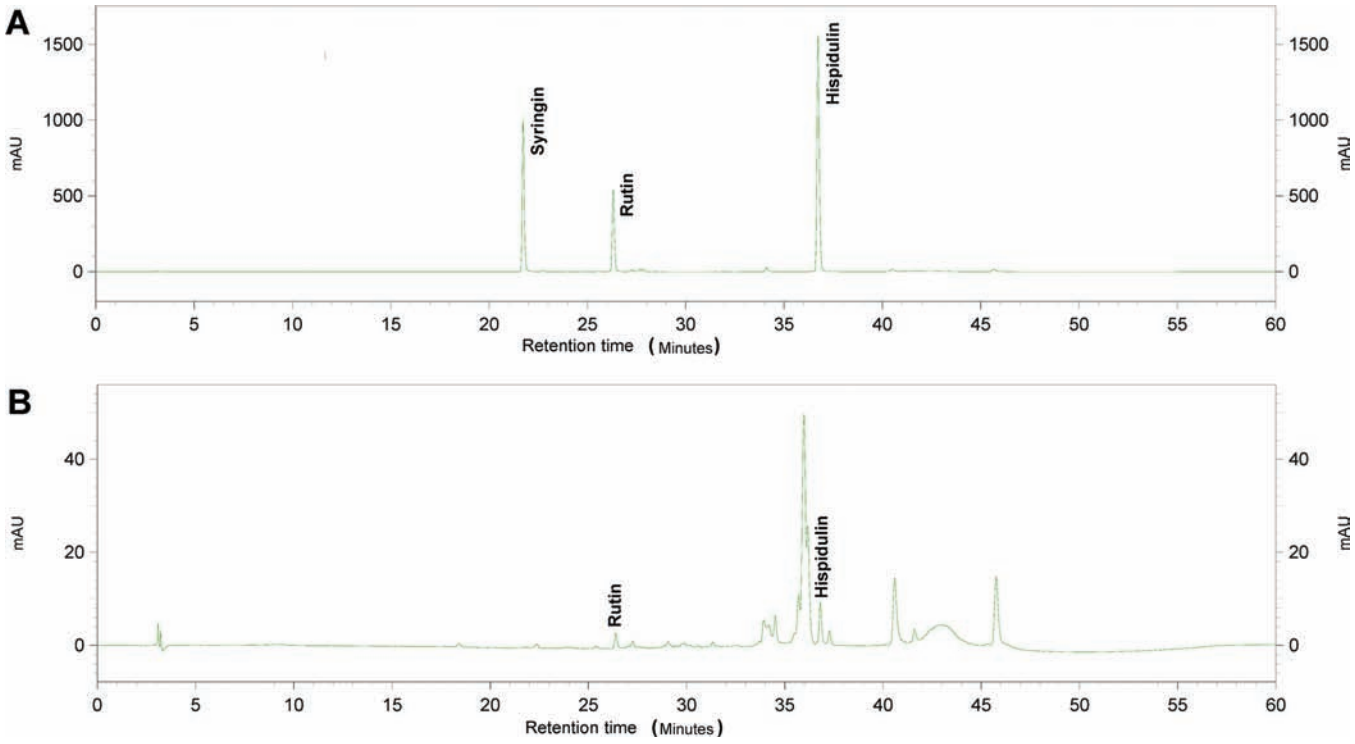

Figure 8. Profile of constituents in SI-2 extracts. (**A**) Mixture of hispidulin, rutin, and syringing. (**B**) The chromatograms of SI-2.

and STAT3 pathways can synergize with, or overcome resistance to, chemotherapy, radiation therapy, and targeted agents in cancer (*30*). Drugs targeted at molecules associated with PI3K/AKT and STAT3 signaling pathways, such as EGFR, are more important than direct inhibitors of the pathway. Importantly, ample evidence suggests that PI3K/AKT inhibition in response to targeting many of these molecules is necessary for therapeutic efficacy. Our observations suggested that *S. involucrata* treatment inhibited phosphorylation of Akt and STAT3. Interestingly, we did an AKT and STAT3 overexpression experiment using cDNA of CA-AKT and CA-STAT3. As our results, the SI-2-treated AKT and STAT3-overexpressing cells showed no enhanced inhibition of cell proliferation, in comparison with the control (**Figure 6B**). The present study suggests that *S. involucrata* might target, at least in part, AKT and STAT3 in the PC3 cells.

The importance of MAPK-signaling pathways in regulating inhibition of cell growth during conditions of stress has been widely investigated (*31*, *32*). The effect of *S. involucrata* on early signal transduction pathways was examined using ERK, p38, and JNK. *S. involucrata* treatment resulted in upregulation of p38 phosphorylation. Previous studies have demonstrated that the MAPK pathway is involved in cell growth inhibition (*33*) and/or the regulation of the cell cycle (*34*). To examine whether *S. involucrata* inhibits cell growth via activation of the p38 pathways, PC3 cells were exposed to SI-2 for 24 h in the absence or presence of SB203580, a specific inhibitor of p38. As shown in **Figure 6D**, treatment with SB203580 had no recovered effect on cell growth inhibition of SI-2. The data further suggest that the induction of apoptosis by *S. involucrata* is not due to further activation of the p38 pathways.

In conclusion, the use of naturally occurring compounds in the development of antitumor agents has become a critical topic in the scientific and industrial communities. *S. involucrata* is a rare traditional Chinese medicinal herb on the verge of extinction. Modern pharmacological studies have demonstrated that it possesses activities such as anticancer. However, the exact molecular mechanisms underlying the cellular effects resulting from *S. involucrata* treatment have yet to be fully explained. To the best of our knowledge, no previous studies have focused on *S. involucrata*-induced cell growth inhibition due to inhibition of EGFR signaling in cancer cells. Taken together, the composite result suggests that *S. involucrata* is an effective inhibitor of EGFR and its downstream signaling molecules, PI3K/AKT and STAT3, at least in prostate cancer and holds great promise for its treatment. It is tempting to suggest that *S. involucrata* could be developed as an agent for the management of EGFR-positive human cancers.

ABBREVIATIONS USED

EGFR, epidermal growth factor receptor; CDK4, cyclin-dependent kinase 4; PI3K, phosphatidylinositol 3-kinase; MAPK, mitogen-activated protein kinase; JNK, c-jun N-terminal kinase; Rb, retinoblastoma; CAM, Complementary and Alternative Medicine; MTT, 3-(4,5-dimethylthiazol-2-yl)-2,5-diphenyl tetrazolium bromide; PI, propidium iodide; FBS, fetal bovine serum.

ACKNOWLEDGMENT

We thank William K. Earl for English editing.

LITERATURE CITED

(1) Fu, L. G. *China Plant Red Data Book—rare and Endangered Plants*; Chinese Science Press: Beijing, 1992; Vol. 1 [M], pp 234−235.
(2) Li, J. S.; Cai, S. Q. Chemical constituents and pharmcological activity of eight species herb Xuelianhua. *Chin. Pharm. J.* **1998**, *33*, 449–452.
(3) Smith, R. A.; Cokkinides, V.; Brawley, O. W. Cancer screening in the United States, 2009: A review of current American Cancer Society guidelines and issues in cancer screening. *CA Cancer J. Clin.* **2009**, *59*, 27–41.
(4) Griffiths, K.; Eaton, C. L.; Harper, M. E.; Turkes, A.; Peeling, W. B. Hormonal treatment of advanced disease: Some newer aspects. *Semin. Oncol.* **1994**, *21*, 672–687.
(5) Ciardiello, F. Epidermal growth factor receptor tyrosine kinase inhibitors as anticancer agents. *Drugs* **2000**, *60* (Suppl. 1), 25–32.

(6) Yarden, Y.; Sliwkowski, M. X. Untangling the ErbB signaling network. *Nat. Rev. Mol. Cell Biol.* **2001**, *2*, 127–137.
(7) Prenzel, N.; Fischer, O. M.; Streit, S.; Hart, S.; Ullrich, A. The epidermal growth factor receptor family as a central element for cellular signal transduction and diversification. *Endocr. Relat. Cancer* **2001**, *8*, 11–31.
(8) Di Lorenzo, G.; Tortora, G.; D'Armiento, F. P.; De Rosa, G.; Staibano, S.; Autorino, R.; D'Armiento, M.; De Laurentiis, M.; De Placido, S.; Catalano, G.; Bianco, A. R.; Ciardiello, F. Expression of epidermal growth factor receptor correlates with disease relapse and progression to androgen-independence in human prostate cancer. *Clin. Cancer Res.* **2002**, *8*, 3438–3444.
(9) Itoh, N.; Patel, U.; Skinner, M. K. Developmental and hormonal regulation of transforming growth factor-alpha and epidermal growth factor receptor gene expression in isolated prostatic epithelial and stromal cells. *Endocrinology* **1998**, *139*, 1369–1377.
(10) Festuccia, C.; Gravina, G. L.; Angelucci, A.; Millimaggi, D.; Muzi, P.; Vicentini, C.; Bologna, M. Additive antitumor effects of the epidermal growth factor receptor tyrosine kinase inhibitor, gefitinib (Iressa), and the nonsteroidal antiandrogen, bicalutamide (Casodex), in prostate cancer cells in vitro. *Int. J. Cancer* **2005**, *115*, 630–640.
(11) Vinals, F.; Chambard, J. C.; Pouyssegur, J. p70 S6 kinase-mediated protein synthesis is a critical step for vascular endothelial cell proliferation. *J. Biol. Chem.* **1999**, *274*, 26776–26782.
(12) Meloche, S.; Pouysségur, J. The ERK1/2 mitogen-activated protein kinase pathway as a master regulator of the G1- to S-phase transition. *Oncogene* **2007**, *26*, 3227–3239.
(13) Polager, S.; Ginsberg, D. E2F—At the crossroads of life and death. *Trends Cell Biol.* **2008**, *18*, 528–535.
(14) Harper, J. W.; Elledge, S. J.; Keyomarsi, K.; Dynlacht, B.; Tsai, L. H.; Zhang, P.; Dobrowolski, S.; Bai, C.; Connell-Crowley, L.; Swindell, E. Inhibition of cyclin-dependent kinases by p21. *Mol. Biol. Cell* **1995**, *6*, 387–400.
(15) Morgan, D. O. Principles of CDK regulation. *Nature* **1995**, *374*, 131–134.
(16) Kuo, P. T.; Lin, T. P.; Liu, L. C.; Huang, C. H.; Lin, J. K.; Kao, J. Y.; Way, T. D. Penta-*O*-galloyl-*β*-D-glucose suppresses prostate cancer bone metastasis by transcriptionally repressing EGF-induced MMP-9 expression. *J. Agric. Food Chem.* **2009**, *57*, 3331–3339.
(17) Way, T. D.; Lin, H. Y.; Kuo, D. H.; Tsai, S. J.; Shieh, J. C.; Wu, J. C.; Lee, M. R.; Lin, J. K. Pu-erh tea attenuates hyperlipogenesis and induces hepatoma cells growth arrest through activating AMP-activated protein kinase (AMPK) in human HepG2 cells. *J. Agric. Food Chem.* **2009**, *57*, 5257–5264.
(18) Li, P.; Nijhawan, D.; Wang, X. Mitochondrial activation of apoptosis. *Cell* **2004**, *116* (Suppl. 2), S57–S59.
(19) Fu, C. X.; Xu, Y. J.; Zhao, D. X.; Ma, F. S. A comparison between hairy root cultures and wild plants of *Saussurea involucrata* in phenylpropanoids production. *Plant Cell Rep.* **2006**, *24*, 750–754.
(20) Li, Y.; Wang, C.; Guo, S.; Yang, J.; Xiao, P. Three guaianolides from *Saussurea involucrata* and their contents determination by HPLC. *J. Pharm. Biomed. Anal.* **2007**, *44*, 288–292.
(21) Chiang, P. C.; Lin, S. C.; Pan, S. L.; Kuo, C. H.; Tsai, I. L.; Kuo, M. T.; Wen, W. C.; Chen, P.; Guh, J. H. Antroquinonol displays anticancer potential against human hepatocellular carcinoma cells: A crucial role of AMPK and mTOR pathways. *Biochem. Pharmacol.* **2010**, *79*, 162–171.
(22) Li, Z. F.; Wang, Z. D.; Ji, Y. Y.; Zhang, S.; Huang, C.; Li, J.; Xia, X. M. Induction of apoptosis and cell cycle arrest in human HCC MHCC97H cells with Chrysanthemum indicum extract. *World J. Gastroenterol.* **2009**, *15*, 4538–4546.
(23) Abbas, T.; Dutta, A. p21 in cancer: intricate networks and multiple activities. *Nat. Rev. Cancer* **2009**, *9*, 400–414.
(24) Khan, N.; Afaq, F.; Mukhtar, H. Apoptosis by dietary factors: the suicide solution for delaying cancer growth. *Carcinogenesis* **2007**, *28*, 233–239.
(25) Fesik, S. W. Promoting apoptosis as a strategy for cancer drug discovery. *Nat. Rev. Cancer* **2005**, *5*, 876–885.
(26) Xiao, X.; Wu, J.; Zhu, X.; Zhao, P.; Zhou, J.; Liu, Q. Q.; Zheng, L.; Zeng, M.; Liu, R.; Huang, W. Induction of cell cycle arrest and apoptosis in human nasopharyngeal carcinoma cells by ZD6474, an inhibitor of VEGFR tyrosine kinase with additional activity against EGFR tyrosine kinase. *Int. J. Cancer* **2007**, *121*, 2095–2104.
(27) Schlessinger, J. Cell signaling by receptor tyrosine kinases. *Cell* **2000**, *103*, 211–225.
(28) Yarden, Y.; Sliwkowski, M. X. Untangling the erbB signaling network. *Nat. Rev. Mol. Cell Biol.* **2001**, *2*, 127–137.
(29) Yu, H.; Jove, R. The STATs of cancer—New molecular targets come of age. *Nat. Rev. Cancer* **2004**, *4*, 97–105.
(30) Hennessy, B. T.; Smith, D. L.; Ram, P. T.; Lu, Y.; Mills, G. B. Exploiting the PI3K/AKT pathway for cancer drug discovery. *Nat. Rev. Drug Discovery* **2005**, *4*, 988–1004.
(31) Lee, E. R.; Kang, Y. J.; Kim, J. H.; Lee, H. T.; Cho, S. G. Modulation of apoptosis in HaCaT keratinocytes via differential regulation of ERK signaling pathway by flavonoids. *J. Biol. Chem.* **2005**, *280*, 31498–31507.
(32) Park, J. I.; Strock, C. J.; Ball, D. W.; Nelkin, B. D. The Ras/Raf/MEK/extracellular signal-regulated kinase pathway induces autocrine-paracrine growth inhibition via the leukemia inhibitory factor/JAK/STAT pathway. *Mol. Cell. Biol.* **2003**, *23*, 543–554.
(33) Moon, S. K.; Jung, S. Y.; Choi, Y. H.; Lee, Y. C.; Patterson, C.; Kim, C. H. PDTC, metal chelating compound, induces G1 phase cell cycle arrest in vascular smooth muscle cells through inducing p21Cip1 expression: Involvement of p38 mitogen activated protein kinase. *J. Cell. Physiol.* **2004**, *198*, 310–323.
(34) Lee, B; Kim, C. H.; Moon, S. K. Honokiol causes the p21WAF1-mediated G(1)-phase arrest of the cell cycle through inducing p38 mitogen activated protein kinase in vascular smooth muscle cells. *FEBS Lett.* **2006**, *580*, 5177–5184.

Received for review October 29, 2009. Revised manuscript received January 20, 2010. Accepted February 9, 2010. This study was supported in part by grants from the National Science Council (NSC-97-2320-B-039-008-MY3) and the China Medical University (CMU98-OC-04, CMU98-S-13, and CMU97-263).